Origin of Size-Dependent Reactivity of Nickel Cluster Ions with Methanol

Ramkuber T. Yadav,[‡,†] Masahiko Ichihashi,[§] and Tamotsu Kondow*[,§]

East Tokyo Laboratory, Genesis Research Institute, Inc., 717-86 Futamata, Ichikawa, Chiba 272-0001, Japan, and Cluster Research Laboratory, Toyota Technological Institute in East Tokyo Laboratory, Genesis Research Institute, Inc., 717-86 Futamata, Ichikawa, Chiba 272-0001, Japan

Received: January 27, 2004; In Final Form: June 8, 2004

Optimized structures of nickel cluster ions, Ni_n^+ ($n = 2-8$), were obtained by use of the density functional method. In comparison with the reaction of a methanol molecule with Ni_n^+ (chemisorption, demethanation and carbide formation), it is revealed that (1) the total reaction (mainly chemisorption) cross section is anti-correlated to the HOMO−LUMO gap of Ni_n^+ and (2) the selectivity of the carbide formation against the demethanation is determined by a propensity, "d-vacancy" (the number of the d-holes per atom); the demethanation proceeds selectively on Ni_n^+ with a d-vacancy of less than about 1.1 and the carbide formation otherwise.

Introduction

Size-specific reactions involving metal clusters have been investigated[1−20] and attempts have been made to correlate the rates of the reactions with various physical properties of the metal clusters exhibiting specific size dependence. At first, Whetten et al. found a strong correlation between the rate of hydrogen dissociative adsorption on an iron cluster and its ionization potential,[5,6] because of cluster-to-hydrogen electron transfer involved in the hydrogen dissociation. Afterward, Conceição et al. and Kietzmann et al. have shown that the rates of the dissociative adsorption of a hydrogen molecule on the clusters of iron, cobalt, nickel, and niobium are correlated with the HOMO-LUMO gaps of the clusters.[10,13]

Recently we studied the reaction of nickel cluster ions, Ni_n^+, with methanol under single collision conditions, and have discovered that the reaction changes dramatically with the size of Ni_n^+; demethanation proceeds preferentially on Ni_4^+, carbide formation on $Ni_{7,8}^+$, and chemisorption on Ni_6^+.[15] In this study, we have shown that the chemisorption is related to the energy barrier between the physisorbed and the chemisorbed states and the selectivity of the carbide formation against the demethanation is determined by the interatomic distance of Ni_n^+.

To search further for the key factors which control the reactivity of a methanol molecule on Ni_n^+, we calculated the electronic and geometrical structures of Ni_n^+ ($n = 2-8$) by using the density functional theory, and compared the results with the reaction cross sections of a methanol molecule on Ni_n^+ measured in our previous study. It was revealed that the total reaction cross section and the selectivity of the reaction are correlated to the HOMO-LUMO gap and the d-vacancy (the number of d-holes per atom), respectively.

Theoretical Background and Computational Procedure

Geometry optimization of nickel cluster ions, Ni_n^+ ($n = 2-8$), with possible spin multiplicities was performed by using the ADF (Amsterdam Density Functional) package developed by Baerends and co-workers.[21]

The self-consistent-field (SCF) equation was solved at a level of the local density approximation (LDA) at each optimization step, and then the energy and its derivatives of the geometry thus optimized were evaluated at a level of the generalized gradient approximation (GGA). Significant errors did not result from exclusion of the GGA terms in the SCF procedure. The exchange and the correlation functionals of LDA are those obtained from parametrization of free electron gas, which Vosko, Wilk, and Nusair (VWN) have derived,[22] while the exchange and the correlation functionals of GGA are those calculated by Becke[23] and Perdew[24] (BP86), respectively. A triple ζ basis set was used to express the atomic orbitals of a nickel atom having the electronic configuration of $4s^1 3d^9$. The frozen core approximation up to the 2p shell was applied.

Computational Results

Geometrical isomers of Ni_n^+ with $n = 2-8$ were optimized in energy, and the electronic states including spin multiplicities were obtained. Figure 1 shows all of the calculated structures of which energies are given below the corresponding structures. In Figure 2, the energy for each size is plotted as a function of the spin multiplicity, M ($=2S + 1$), and in Figure 3, the details of the structures in the ground states are exhibited.

Ni_2^+. A nickel dimer cation, Ni_2^+, in the lowest energy state obtained in the calculation (defined as the ground state) has a spin multiplicity, M, of 4 with an equilibrium interatomic distance, R_e, of 2.30 Å. The second lowest state having $M = 2$ with $R_e = 2.17$ Å is located at an energy higher by 0.30 eV than that of the ground state ($M = 4$).

The reliability of the present calculation is confirmed by the comparison of the present results with other experimental[25−31] and theoretical[32−36] ones of Ni_2^+. For instance, Brucat and co-workers have measured the accurate interatomic distance, R_0 ($=2.242 \pm 0.001$ Å), of Ni_2^+ by use of the rotationally resolved photodissociation spectroscopy.[30] Salahub and co-workers have used the density functional theory at a GGA level (BP86),[35] and have concluded that the ground state has $M = 4$ with an interatomic distance of $R_e = 2.22$ Å and that the $M = 2$ state

* Address correpondence to this author.
‡ East Tokyo Laboratory, Genesis Research Institute, Inc..
† Current address: Research Center, Philip Morris USA.
§ Cluster Research Laboratory, Toyota Technological Institute in East Tokyo Laboratory, Genesis Research Institute, Inc.

10.1021/jp0400723 CCC: $27.50
Published on Web 08/07/2004

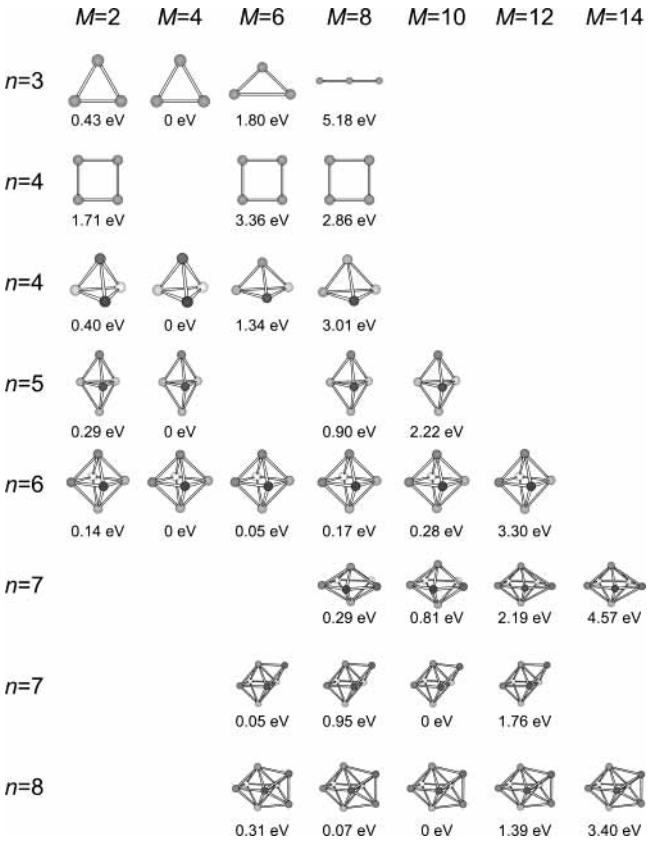

Figure 1. Structures and energies of Ni_n^+ ($n = 3-8$). The value M ($=2S + 1$) shows the spin multiplicity of a given electronic state. The values written below the structures show the energies with respect to the energy of the ground state.

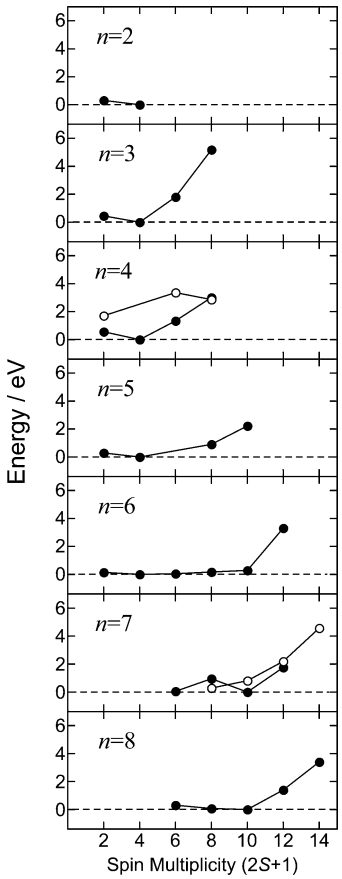

Figure 2. Energies of Ni_n^+ in the ground and the excited electronic states as a function of the spin multiplicity, $2S + 1$. The energies of the ground states are set to zero. In the $n = 4$ graph, the solid and the open circles represent the energies of the tetrahedral and the square isomers, respectively. In the $n = 7$ graph, the solid and the open circles represent the energies of the one-atom capped octahedral and the pentagonal bipyramid isomers, respectively.

with $R_e = 2.25$ Å is located higher by 0.32 eV than the ground state. Recently Gutsev and Bauschlicher have calculated Ni_2^+ thoroughly by use of the density functional theory with six GGA's for the exchange-correlation potential,[36] and have concluded that Ni_2^+ has a $^4\Delta_g$ state in the ground state. The interatomic distance is 2.27 Å in one of the exchange-correlation potentials (BP86) they used. It is concluded, therefore, that the present method is applicable to the calculation for larger nickel cluster ions.

Ni_3^+. A trimer cation, Ni_3^+, has four electronic states with $M = 2$, 4, 6, and 8; Ni_3^+ in the ground state ($M = 4$) has an equilateral triangle structure with the interatomic distance of 2.22 Å. The second lowest state with $M = 2$ is located at 0.43 eV above the ground state; Ni_3^+ in this state has a triangle (close to isosceles) structure with the interatomic distances of 2.18, 2.19, and 2.23 Å. The third ($M = 6$, C_{2v}) and the fourth lowest states ($M = 8$, $D_{\infty h}$) are located at 1.80 and 5.18 eV above the ground state, respectively. Salahub and co-workers have reported that Ni_3^+ in the ground state ($M = 4$) has a quasiequilateral triangle structure with the interatomic distances of 2.30, 2.30, and 2.31 Å, and the second lowest state ($M = 2$) is located at 0.25 eV above the ground state.[35] Their result is consistent with the present calculation.

Ni_4^+. A tetramer cation, Ni_4^+, has two geometrical isomers with tetrahedral and square structures. The tetrahedral isomer has four electronic states with $M = 2$, 4, 6, and 8, in the energy spread of $\approx$3 eV; the isomer having a regular tetrahedral structure (interatomic distance of 2.25 Å) with $M = 4$ is in the ground state. There is the second lowest state with $M = 2$ having a distorted tetrahedral structure (interatomic distances of 2.23−2.29 Å) located at 0.40 eV above the ground state. The structures are distorted at a higher extent in $M = 6$ and 8. On the other hand, the isomers with square structures have the lowest energy state at $M = 2$, whose energy is 1.71 eV above the energy of the tetrahedral isomer in the ground state. Salahub and co-workers have reported that Ni_4^+ in the ground state has a regular tetrahedral structure with interatomic distances of 2.30 Å,[35] which are slightly longer than those obtained in the present calculation.

Ni_5^+. There are four electronic states with $M = 2$, 4, 8, and 10 in a pentamer cation, Ni_5^+. The ground state ($M = 4$) has a trigonal bipyramid structure with interatomic distances of 2.27−2.31 Å. The second lowest state is located at 0.29 eV above the ground state, and Ni_5^+ in this state has a similar trigonal bipyramid structure. Another state with $M = 10$ is located at 2.22 eV in energy above the ground state. The $M = 10$ state has the highest energy obtained in the present calculation. The interatomic distances of Ni_5^+ are slightly longer than those of Ni_3^+ and Ni_4^+.

Ni_6^+. Five electronic states out of the six electronic states obtained have energies within 0.28 eV with spin multiplicities of $M = 2-10$: the lowest energy state with $M = 4$ and the highest energy state with $M = 12$. The cluster ion, Ni_6^+, in the lowest energy electronic state ($M = 4$) has a compressed octahedral structure having a nearest neighbor distance of 2.28 Å and a ratio of the lengths of the shorter and the longer axes of 0.96, while that in the second lowest state ($M = 6$) has a less symmetric octahedral structure whose energy is higher by 0.05 eV than that of the ground state.

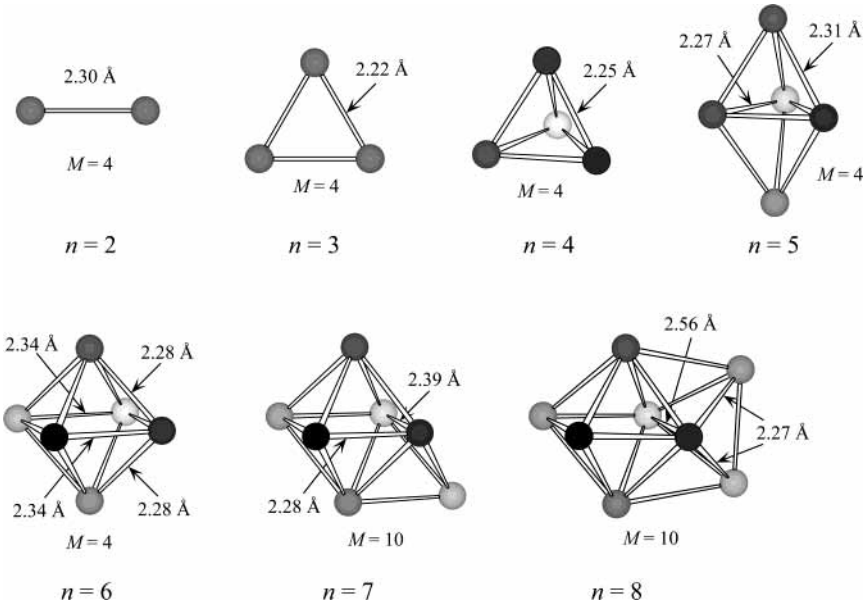

Figure 3. Structures of Ni_n^+ ($n = 2-8$) in their ground states. The value M ($=2S + 1$) shows the spin multiplicity of a given electronic state. The longest and the shortest bond lengths are written beside the structures.

Ni_7^+. It is shown by calculation that Ni_7^+ possesses nine electronic states including geometrical isomers with $M = 6-14$. The structure of Ni_7^+ in the ground state ($M = 10$) is a one-atom capped octahedral structure with interatomic distances between 2.28 and 2.39 Å, and Ni_7^+ in the second lowest electronic state ($M = 6$) is located at 0.05 eV above the ground state, and has almost the same structure. In addition, Ni_7^+ having pentagonal bipyramid structures are found to be stable; among them the electronic state with $M = 8$ has the lowest energy, which is higher by 0.29 eV than that of the ground state.

Ni_8^+. Among the five electronic states of Ni_8^+ with $M = 6-14$ obtained, the ground state has a spin multiplicity of $M = 10$ and a two-atom capped octahedral structure with the shortest and the longest interatomic distances of 2.27 and 2.56 Å, respectively. The $M = 6$ and 8 states are located at 0.31 and 0.07 eV above the ground state, while the $M = 12$ and 14 states are 1.39 and 3.40 eV above it.

Discussion

Bond Dissociation Energy. To examine the reliability of the present calculation, the bond dissociation energies of Ni_n^+ ($Ni_n^+ \rightarrow Ni_{n-1}^+ + Ni$) were calculated. Under the constraint of the spin conservation, Ni_n^+ in the ground state ($M = m$) should dissociate into Ni_{n-1}^+ ($M = m - 2$, m, or $m + 2$) and Ni in the ^3D ($4s^13d^9$) or ^3F ($4s^23d^8$) state. In this calculation, (1) the energy of the releasing Ni atom is represented by the energy of the ^3D state because the energies of the ^3D and the ^3F states are almost the same, and (2) the zero-point energy is ignored. The minimum energy difference between Ni_n^+ in the ground state and $Ni_{n-1}^+ + Ni$ in the above assumptions was adopted as the bond dissociation energy of Ni_n^+, as shown in Figure 4. The calculated dissociation energies are consistently higher by about 1 eV than the experimental dissociation energies,[25,26] though the bond dissociation energy of Ni_2^+ calculated by the present method agrees reasonably well with that calculated in ref 36. One concludes, beside the systematic deviation of 1 eV, that the calculation predicts well the experimental size dependence of the dissociation energy.

HOMO-LUMO Gap and Total Reaction. Figure 5 shows the energy gaps between the highest occupied molecular orbital (HOMO) and the lowest unoccupied molecular orbital (LUMO) of Ni_n^+ in the ground and several low-lying states. The HOMO-LUMO gaps were calculated without orbital relaxation, and they tend to be smaller than those with orbital relaxation or those in the Hartree−Fock approximation. As shown in Figures 1 and 2, the present calculation reveals several low-lying excited states of Ni_n^+. Among them, we show in Figure 5 the HOMO-LUMO gaps involving the low-lying states whose energy difference from the ground state is smaller than 1 eV. As the internal temperature of Ni_n^+ is about 300 K, isomers having higher energies are not involved in the reactions; these isomers should be taken into consideration if they have high densities of states in the phase space. Evidently, $Ni_{5,6}^+$ have lower HOMO-LUMO gaps than those of Ni_4^+ or $Ni_{7,8}^+$ in the ground state, and even if the contribution from the low-energy excited states is not negligible, still $Ni_{5,6}^+$ have lower HOMO-LUMO gaps than that of Ni_4^+. As shown in Figure 5, the HOMO-LUMO gap is anti-correlated to the total reaction cross section; the total reaction cross section is largest at a size of 6 and smallest at a size of 4, while the HOMO-LUMO gap is smallest at a size of 6 and largest at a size of 4. In our previous study on the reaction of Ni_n^+ with a methanol molecule, we have evaluated the size dependence of the energy barrier from the experimental reaction cross sections.[15] The activation barrier arises from Pauli repulsion between the valence electrons of the reactant molecule

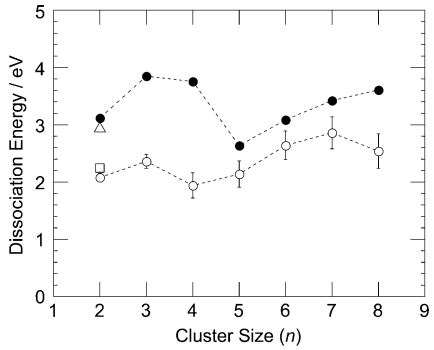

Figure 4. Bond dissociation energies as a function of the cluster size, n. Solid circles show the calculated values in the present study. Open circles show the experimental values in refs 26 and 27. The open square shows the experimental value in ref 30. The open triangle shows the calculated (BP86) value in ref 36.

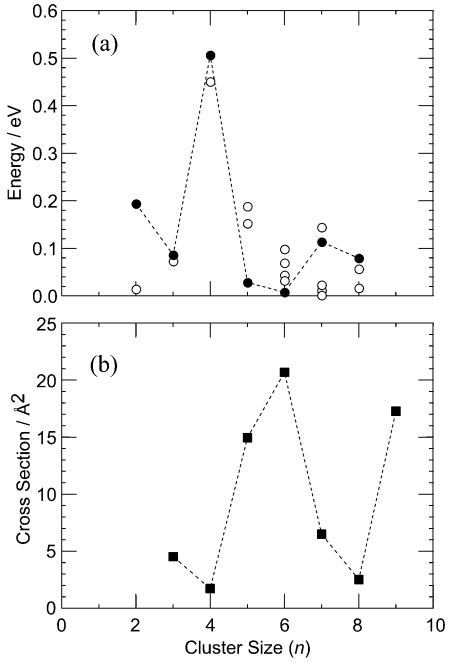

Figure 5. The calculated HOMO-LUMO gap [panel a] and the experimental reaction cross section for $Ni_n^+ + CH_3OH$ [panel b] are plotted as a function of the cluster size (ref 15). In panel a, the solid circles show the HOMO-LUMO gaps for nickel cluster ions in the ground states, and the open circles show those in the low-lying states. The energy differences between the ground and the low-lying states are less than 1 eV.

and the cluster ion. The height of this energy barrier is approximated by the energy of electron promotion from HOMO to LUMO. Our present calculation suggests that this mechanism explains the reaction between Ni_n^+ and a methanol molecule. Similarly, Conceição et al.[10] and Kietzmann et al.[13] have reported that the size-dependent reactivities of the neutral iron, cobalt, nickel, and niobium clusters with a hydrogen molecule exhibit a clear correlation to the size-dependent HOMO-LUMO gaps; the reaction proceeds if the system overcomes the energy barrier of the hydrogen activation.

d-Vacancy: Demethanation vs. Carbide Formation. As described in our previous study on the reaction of a nickel cluster ion with a methanol molecule, the reaction is remarkably size selective; demethanation proceeds preferentially at a size of 4, chemisorption at a size of 6, and carbide formation at sizes of 7 and 8. Actually, the present calculation showed that the size-dependent reaction selectivity appears to be related to the spin multiplicity of the nickel cluster ion, Ni_n^+; Ni_n^+ ($n \leq 6$) have a spin multiplicity of 4, while Ni_n^+ ($n \geq 7$) have a spin multiplicity of 10. To examine how the reaction selectivity changes with the spin multiplicity, the electronic structures of Ni_4^+ ($M = 4$ and 6) were calculated and were compared with the corresponding cluster ions, $Ni_4^+(CH_3OH)$, in which CH_3OH is chemisorbed undissociatively through the Ni−O bond. The calculation provides the following results: In both cluster ions with spin multiplicities of $M = 4$ and 6, the oxygen atom of the methanol molecule donates p-electrons to the bonding nickel atom, and hence more p-electrons are distributed in the vicinity of the nickel atom, when a methanol molecule is chemisorbed to the cluster ion. Upon chemisorption of a methanol molecule on a cluster ion with $M = 4$, d-electrons are transferred mainly from the oxygen-bonded nickel atom to a free nickel atom, while upon chemisorption on that with $M = 6$ s-electrons are transferred and are localized on one of the neighboring nickel atoms. It is likely that the carbon atom of the chemisorbed methanol molecule attacks an s-electron rich or a d-electron poor atom because s-electrons are delocalized. These findings suggest that the d-vacancy concept is applicable to reactions occurring on metal clusters or ions; it is well-known that the rate of a catalytic reaction on a transition-metal surface is closely related to the d-vacancy of the constituent metal atom (the number of d-electron holes per metal atom).[37,38] Figure 6 shows the calculated d-vacancy of Ni_n^+ as a function of the cluster size, n, in comparison with size dependence of the cross sections for the demethanation and the carbide formation. Evidently, the demethanation and the carbide formation exhibit anti-correlation and correlation to the d-vacancy, respectively; the demethanation is favored on a cluster ion with a d-vacancy smaller than about 1.1 and the carbide formation otherwise except for Ni_3^+. In Ni_3^+, a geometrical effect may impede the carbide formation; in the reaction intermediate, $Ni_3^+(CH_3OH)$, the carbon atom is much more distant to an available nickel atomic site than that in $Ni_{7,8}^+(CH_3OH)$ so that the carbon atom has a lesser chance to bind to the nickel site to form a carbide.

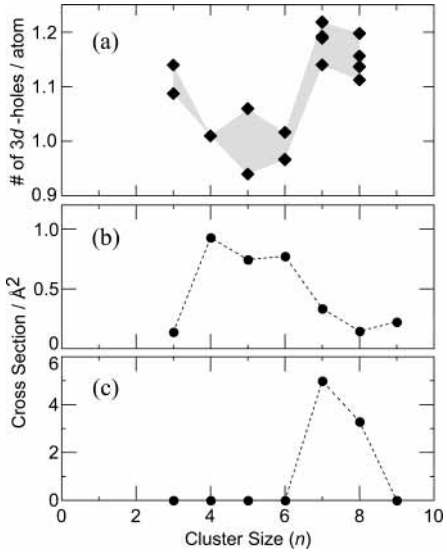

Figure 6. A number of 3d-electron holes for each constituent atom of the most stable Ni_n^+ [panel a] and experimental cross sections for the production of Ni_nO^+ [panel b] and $Ni_{n-1}C^+$ [panel c], respectively,[15] as a function of the cluster size.

Summary

The structures and the energies of Ni_n^+ ($n = 2-8$) were calculated by use of the density functional method. It was revealed that the relationship between the calculated HOMO-LUMO gap and cluster size shows an anti-correlation with that between the reaction cross section of Ni_n^+ with a methanol molecule and the cluster size, n. This anti-correlation is understandable, because the electron promotion energy is correlated with the activation energy barrier. It was also found that the d-vacancy of Ni_n^+ has a relationship with the reaction selectivity between the demethanation and the carbide formation from the chemisorbed methanol molecule; the presence of the relation implies that the d-electrons are involved in forming the chemisorption bond between Ni_n^+ and the methanol molecule.

Acknowledgment. M.I. would like to thank Prof. Y. Ozaki for helpful discussion.

References and Notes

(1) Irion, M. P. *Int. J. Mass Spectrom. Ion Processes* **1992**, *121*, 1.
(2) Knickelbein, M. B. *Annu. Rev. Phys. Chem.* **1999**, *50*, 79.

(3) Bondybey, V. E.; Beyer, M. K. *J. Phys. Chem. A* **2001**, *105*, 951.
(4) Zemski, K. A.; Justes, D. R.; Castleman, A. W., Jr. *J. Phys. Chem. B* **2002**, *106*, 6136.
(5) Whetten, R. L.; Cox, D. M.; Trevor, D. J.; Kaldor, A. *Phys. Rev. Lett.* **1985**, *54*, 1494.
(6) Whetten, R. L.; Zakin, M. R.; Cox, D. M.; Trevor, D. J.; Kaldor, A. *J. Chem. Phys.* **1986**, *85*, 1697.
(7) Elkind, J. L.; Weiss, F. D.; Alford, J. M.; Laaksonen, R. T.; Smalley, R. E. *J. Chem. Phys.* **1988**, *88*, 5215.
(8) Nonose, S.; Sone, Y.; Onodera, K.; Sudo, S.; Kaya, K. *J. Phys. Chem.* **1990**, *94*, 2744.
(9) Sharpe, P.; Campbell, J. M.; Cassady, C. J. *Organometallics* **1994**, *13*, 3077.
(10) Conceição, J.; Laaksonen, R. T.; Wang, L.-S.; Guo, T.; Nordlander, P.; Smalley, R. E. *Phys. Rev. B* **1995**, *51*, 4668.
(11) Dietrich, G.; Dasgupta, K.; Kuznetsov, S.; Lützenkirchen, K.; Schweikhard, L.; Ziegler, J. *Int. J. Mass Spectrom. Ion Processes* **1996**, *157*/*158*, 319.
(12) Vajda, Š.; Wolf, S.; Leisner, T.; Busolt, U.; Wöste, L. H. *J. Chem. Phys.* **1997**, *107*, 3492.
(13) Kietzmann, H.; Morenzin, J.; Bechthold, P. S.; Ganteför, G.; Eberhardt, W. *J. Chem. Phys.* **1998**, *109*, 2275.
(14) Heiz, U.; Sanchez, A.; Abbet, S.; Schneider, W.-D. *J. Am. Chem. Soc.* **1999**, *121*, 3214.
(15) Ichihashi, M.; Hanmura, T.; Yadav, R. T.; Kondow, T. *J. Phys. Chem. A* **2000**, *104*, 11885.
(16) Liu, F.; Liyanage, R.; Armentrout, P. B. *J. Chem. Phys.* **2002**, *117*, 132.
(17) Zakin, M. R.; Brickman, R. O.; Cox, D. M.; Reichmann, K. C.; Trevor, D. J.; Kaldor, A. *J. Chem. Phys.* **1986**, *85*, 1198.
(18) Knickelbein, M. B. *J. Chem. Phys.* **1996**, *104*, 3517.
(19) Knickelbein, M. B.; Koretsky, G. M. *J. Phys. Chem. A* **1998**, *102*, 580.
(20) Rousseau, R.; Dietrich, G.; Krückeberg, S.; Lützenkirchen, K.; Marx, D.; Schweikhard, L.; Walther, C. *Chem. Phys. Lett.* **1998**, *295*, 41.
(21) *Amsterdam Density Functional*, v. 2.3.0: Baerends, E. J.; Ellis, D. E.; Ros, P. *Chem. Phys.* **1973**, *2*, 41. te Velde, G.; Baerends, E. J. *J. Comput. Phys.* **1992**, *99*, 84. Fonseca Guerra, C.; Visser, O.; Snijders, J. G.; te Velde, G.; Baerends, E. J. In *Parallelisation of the Amsterdam Density Functional Programme, in Methods and Techniques for Computational Chemistry*; Clementi, E., Corongiu, G., Eds.; STEF: Cagliari, 1995.
(22) Vosko, S. H.; Wilk, L.; Nusair, M. *Can. J. Phys.* **1980**, *58*, 1200.
(23) Becke, A. D. *Phys. Rev. A* **1988**, *38*, 3098.
(24) Perdew, J. P. *Phys. Rev. B* **1986**, *33*, 8822.
(25) Lessen, D.; Brucat, P. J. *Chem. Phys. Lett.* **1989**, *160*, 609.
(26) Lian, L.; Su, C.-X.; Armentrout, P. B. *Chem. Phys. Lett.* **1991**, *180*, 168.
(27) Lian, L.; Su, C.-X.; Armentrout, P. B. *J. Chem. Phys.* **1992**, *96*, 7542.
(28) Asher, R. L.; Bellert, D.; Buthelezi, T.; Brucat, P. J. *Chem. Phys. Lett.* **1994**, *224*, 525.
(29) Asher, R. L.; Bellert, D.; Buthelezi, T.; Brucat, P. J. *Chem. Phys. Lett.* **1994**, *224*, 529.
(30) Bellert, D.; Buthelezi, T.; Lewis, V.; Dezfulian, K.; Reed, D.; Hayes, T.; Brucat, P. J. *Chem. Phys. Lett.* **1996**, *256*, 555.
(31) Buthelezi, T.; Bellert, D.; Lewis, V.; Dezfulian, K.; Kisko, J.; Hayes, T.; Brucat, P. J. *Chem. Phys. Lett.* **1996**, *257*, 340.
(32) Upton, T. H.; Goddard, W. A., III *J. Am. Chem. Soc.* **1978**, *100*, 5659.
(33) Bauschlicher, C. W., Jr.; Partridge, H.; Langhoff, S. R. *Chem. Phys. Lett.* **1992**, *195*, 360.
(34) Merchán, M.; Pou-Amérigo, R.; Roos, B. O. *Chem. Phys. Lett.* **1996**, *252*, 405.
(35) Cisneros, G. A.; Castro, M.; Salahub, D. R. *Int. J. Quantum Chem.* **1999**, *75*, 847.
(36) Gutsev, G. L.; Bauschlicher, C. W., Jr. *J. Phys. Chem. A* **2003**, *107*, 4755.
(37) Beeck, O. *Discuss. Faraday Soc.* **1950**, *8*, 118.
(38) Boudart, M. *J. Am. Chem. Soc.* **1950**, *72*, 1040.